Positron Scattering and Annihilation Studies Using a Trap-Based Beam

L. D. Barnes, J. P. Marler, J. P. Sullivan* and C. M. Surko**

Department of Physics, University of California, San Diego, La Jolla CA, 92093; USA

Abstract

An overview is presented of recent studies of the interaction of low-energy positrons with atoms and molecules using a trap-based positron beam. The beam is tunable from $\sim 100\,\text{meV}$ to many electron volts, with a typical energy resolution of 25 meV (FWHM). A variety of scattering processes are investigated using the properties of positron orbits in a spatially varying magnetic field. Recent scattering measurements are reviewed, and new data for electronic excitation, ionization, and positronium formation in noble gases are presented. In a separate set of experiments, positron annihilation below the threshold for positronium formation is studied in molecules as a function of positron energy. The data show large Feshbach resonances in the range of energies of the molecular vibrations. Within the framework of this model, these results provide the first experimental evidence that positrons bind to hydrocarbon molecules.

1. Introduction

Positron interactions with atoms and molecules pose a number of challenges to our fundamental understanding of atomic physics [1,2]. Examples include developing methods to treat electron-positron correlations and the process of positronium formation, either as an open or closed channel. One focus of interest is the four-decade-old problem of positron annihilation in large molecules, where annihilation rates can be orders of magnitude greater than that expected on the basis of simple collisions [3–7]. Other topics of interest include positron-impact ionization, excitation of electronic transitions in atoms and molecules, and vibrational excitation of molecules [8–10]. Developing a quantitative understanding of low-energy positron interactions with matter can also aid greatly in areas such as condensed matter physics and gamma-ray astronomy [11,12]. Technological applications include developing new methods for mass spectroscopy and the characterization of materials using positrons [13]. Following a brief overview of recent studies of positron scattering using a trap-based beam, new data are presented for electronic excitation, ionization and positronium formation in noble gases. Experiments to study positron annihilation in molecules below the threshold for positronium formation are described. The data show large enhancements in annihilation rate at energies near to, but downshifted in energy from the vibrational modes. These results are interpreted in terms of vibrational Feshbach resonances [7]. The results provide evidence that positrons bind to alkane molecules (C_nH_{2n+2}) larger than ethane,

* Present address: Photon Factory, KEK, Tsukuba, Japan.
** Corresponding author, E-mail: csurko@ucsd.edu

with binding energies ranging from $\sim 30\,\text{meV}$ in butane (C_4H_{10}) to 220 meV in dodecane ($C_{12}H_{26}$).

2. Experimental tools

Cold positron beam. The enabling tool used in this work is a state-of-the-art, cold, trap-based positron beam. Positrons from a ^{22}Na source are slowed to a few electron Volts using a solid neon moderator and injected into a Penning–Malmberg trap in the presence of an applied magnetic field, $B \sim 0.1\,\text{T}$ and a molecular nitrogen buffer gas. The accumulator has three stages, each with successively lower gas pressure and electrostatic potential. Following a series of inelastic collisions, the positrons are trapped with an efficiency $\sim 25\%$ in the third stage where the pressure is lowest [14]. The positrons cool to the ambient temperature ($300\,\text{K} = 25\,\text{meV}$) on a mixture of N_2 and CF_4, the latter added for rapid cooling. The schematic arrangement for the formation of the cold beam from the third stage of the positron trap is shown in Fig. 1. After the positrons are accumulated and cooled, they are forced over a fixed-height potential barrier, guided by the B field. This sets the energy of the beam at $E = eV_B$. The energy distribution of the positrons in the direction parallel to the magnetic field is measured using a retarding potential analyzer (RPA). To prevent space charge effects from increasing the beam energy spread, the beam is run in a pulsed mode, producing bursts of $\sim 5 \times 10^4$ positrons at a 4 Hz rate [9]. Typical parallel energy resolution of the beams used for scattering and annihilation studies is approximately the ambient temperature, 25 meV, with a comparable energy spread perpendicular to B.

Scattering in a magnetic field. Since the cold beam is formed in a magnetic field, we have found it both convenient and advantageous to also study scattering in a magnetic field [15]. This is in contrast to the more conventional use of either an electrostatic beam or a weak magnetic guide field. As shown in Fig. 1, the positron beam passes through the gas cell, where the incident beam energy is $e(V_B - V_C)$. The parallel energy of the transmitted beam, consisting of both scattered and unscattered particles, is then analyzed using the RPA.

In the B field, with the exception of the short time during scattering events, the quantity $E_\perp/B$ is an adiabatic invariant, where $E_\perp$ is the energy of the positron due to the velocity components perpendicular to B. The total energy of the positron is $E = E_\parallel + E_\perp$, where $E_\parallel$ is the energy in the motion parallel to B. Elastic scattering converts $E_\parallel$ into $E_\perp$ at constant E. Thus, when no *inelastic*
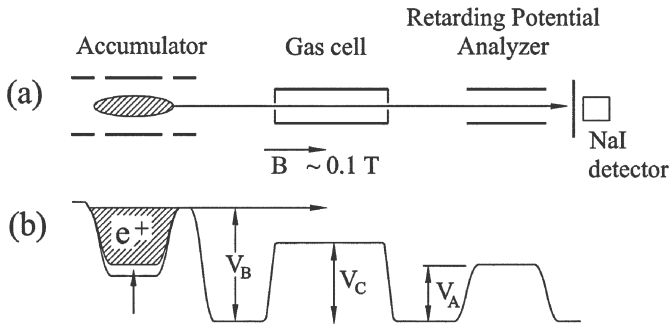
Fig. 1. (a) Schematic diagram of the apparatus to form a cold positron beam and to study scattering in a magnetic field; (b) the corresponding potential profile.

scattering is present, measurement of $E_\parallel$ determines the scattering angle by $\theta = \cos^{-1}[(E_\parallel/E)^{1/2}]$. When both elastic and inelastic scattering are present, the parallel energy distributions of the two processes can overlap. However, if the magnetic field ratio, M, between the field at the scattering cell and the field at the RPA is > 1, then $E_\perp$ is reduced by this ratio, and the spread in parallel energy caused by scattering at an angle can be greatly reduced. This technique permits inelastic and elastic scattering to be distinguished with good resolution by the RPA. The gas cell is 38 cm long with small entrance and exit apertures, and so the pressure and path length in the cell are accurately determined. The absolute, integral cross section for an inelastic process can then be measured by the ratio of step height in the RPA curve (c.f., inset, Fig. 2) to the intensity of the incident positron beam.

Annihilation resolved as a function of positron energy. Using the cold, magnetically guided positron beam, we developed a new method to study positron annihilation, resolved as a function of positron energy [16]. As shown in Fig. 3, the beam passes through a cell containing the test gas. The positrons annihilate with electrons in the test gas, producing gamma-ray photons that are detected using a CsI scintillator. To eliminate the background signal that would arise from positrons colliding with the vacuum chamber or a beam dump, the beam is kept in flight, bouncing back and forth through the gas cell, during the
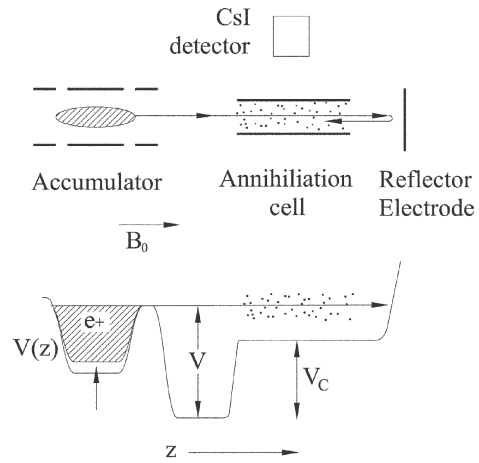

Fig. 2. Cross sections for the ν_2 and ν_3 vibrational modes of CO_2, open and closed circles, respectively [9]. Solid and dashed lines are theory of Kimura *et al.* [26], with no fitted parameters. Inset: RPA data showing steps for both modes.

Fig. 3. Experimental arrangement to measure energy-resolved annihilation rates with the cold positron beam.

time, Δt, that annihilation events are counted (e.g., $\Delta t \sim 15\,\mu s$). In addition, the annihilation cell and gamma-ray detector are surrounded by the shielding equivalent of 5 cm of lead. Using these techniques, the background signal is reduced to approximately 1 count per 10^9 positrons through the cell, while the signal level is typically a factor of 100 larger.

The experiment is run in the single-count regime with pressures adjusted to produce approximately one detected gamma ray for every five pulses of the positron beam. Data sets typically require 16 hours for spectra measured at ~ 50 energies. The statistical uncertainty in Z_{eff} is typically $\sim 1\%$, and systematic uncertainties are $\sim 15\%$.

3. Positron scattering from atoms and molecules

Using the new scattering apparatus, we conducted a number of positron scattering experiments on atomic and molecular targets.

Differential elastic cross sections. We measured differential cross sections at energies below the thresholds for inelastic processes [15,17,18]. At present, the technique measures both back and forward scattering together, yielding cross sections "folded" in scattering angle, θ, about $\theta = 90°$ [15]. This technique yields absolute cross sections with excellent resolution at small values of positron energies, and so it is complementary to conventional methods. Differential cross sections for noble gases are in good agreement with available theoretical calculations.

Vibrational excitation of molecules. We measured the first integral cross sections as a function of positron energy for vibrational excitation of molecules, studying to date CO, H_2, CO_2, and CH_4 [9,18]. These experiments and the early demonstration experiment [17] are the first state-resolved measurements of vibrational excitation of molecules by positron impact. The results for CO_2 are shown above in Fig. 2. Theoretical predictions (available over some of the range of energies for all molecules except N_2) range from fair to excellent agreement with the measurements, with no fitted parameters. Many of the cross sections exhibit sharp increases near threshold that will be the subject of further study.
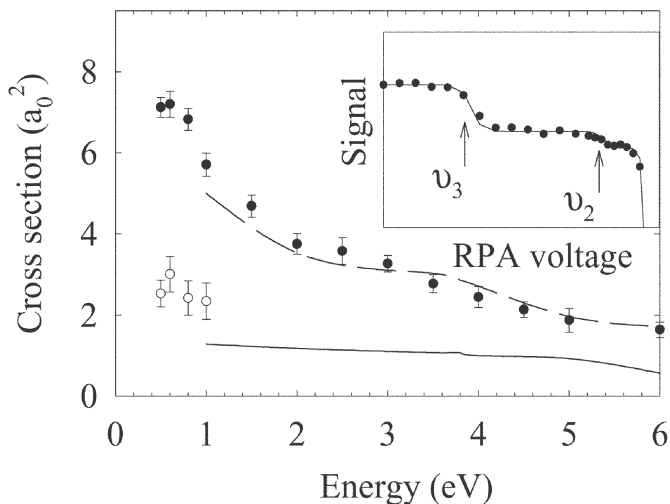
Electronic excitation of atoms and molecules. We studied the excitation of low-lying electronic states of atoms and molecules by positron impact, measuring cross sections for Ar, Xe, H_2, N_2 [10]. In Ar, the largest discrepancies were near threshold, where the theoretical treatment is thought to be less accurate. There was no evidence of the excitation of triplet (i.e., metastable) states, which for positrons is thought to occur only via the spin-orbit interaction (in the absence of the exchange interaction typical in electron scattering). Shown in Fig. 4 are new data for the 6s 3/2 state of xenon, compared with a recent calculation. The data appear to be lower than the predictions by approximately a factor of two. Whether there is a discrepancy near threshold in Xe awaits a more refined measurement.

In molecules, a manifold of vibrational state is associated with each electronic transition, and the known Franck–Condon factors were used to deduce the electronic excitation cross sections. In H_2, the measurements were able to distinguish between two different theories. We studied the lowest lying excited electronic states in N_2. A sharp rise in the $a^1\Pi$ cross section is observed near threshold. This appears to explain the observation that N_2 is the most efficient gas for operation of buffer-gas positron traps. We plan to study this feature in more detail. An important feature of the positron cross sections measurements is that they are fully comparable in quality to available electron data {c.f. Figs. 5(a) c.f. Ref. [19]}. See Ref. [10,18] for details.

Positronium atom formation and ionization. We have now begun to study positronium atom formation by measuring directly the positrons lost from the beam [15]. Since the positrons follow the magnetic field lines and are trapped between the potential barrier, V_B and the detector, when the RPA is placed at zero potential, all positrons that have not annihilated are measured by the detector. Since the direct annihilation is negligible, the number of positrons lost from the beam provides an accurate measure of the positronium formation cross section. Since the pressure and path length are known, this method provides an absolute measure of the cross section.

Using a variant of the technique described above to study vibrational and electronic excitations, we have also
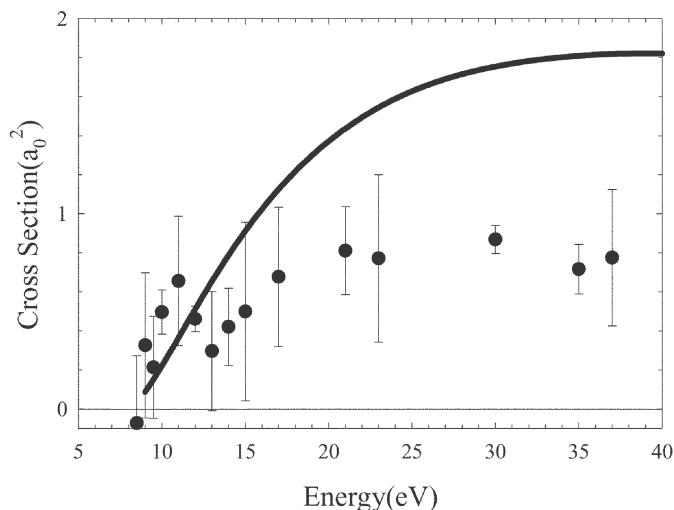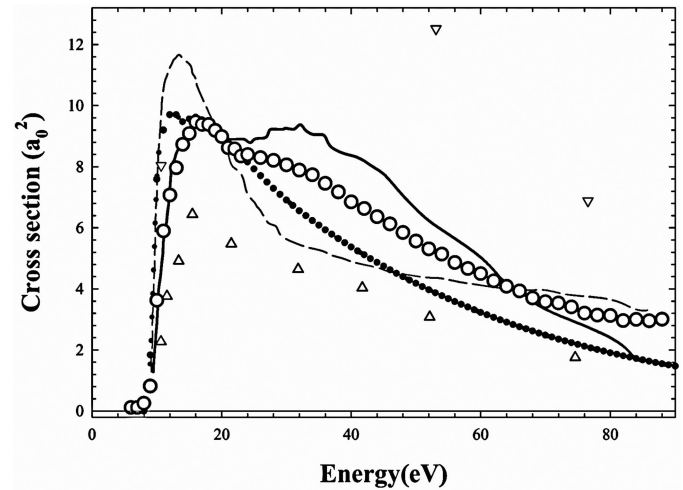

Fig. 5. Absolute positronium formation cross sections for argon: current data (○) previous measurements from Ref. [8] (–); lower (△) and upper (inverted △) limits from a third experiment [28]; and theory of Ref. [20] (●●●). Also shown is comparison with a more recent calculation [21] (---), but this calculation is scaled by a factor of 0.5. For the current data (○) the error bars are smaller than the symbol size. Between 10 and 50 eV, the upper limits of Ref. [28] (inverted △) are off scale.

begun to measure ionization cross sections. Since both the positronium and ionization measurements yield absolute cross sections, they provide an attractive alternative to other current methods of measuring these cross sections (e.g., that require normalization, such as reference to the analogous electron cross sections at very high energies). The ability to make absolute cross section measurements is particularly important in positronium formation, since there is no analogous electron-impact process.

Data for the positronium formation cross section in argon is shown in Fig. 5. An absolute comparison with recent measurements made using a different technique is also shown. In particular, the data of Ref. [8] were obtained from the difference between measurements of the total ionization cross section and the direct ionization cross section (i.e. for the latter process, the positron and ionized electron both remain as free particles at the end of the interaction.) We regard the relatively close agreement between the data sets as encouraging. However, the comparison indicates that the question of a second peak and/or pronounced shoulder around 30 eV warrants further investigation. Figure 5 shows an absolute comparison with the predictions of a theory using the static-exchange approximation to calculate the cross section for formation of ground state positronium [20]. Also shown in the figure are the predictions of a more recent calculation (scaled by 0.5) that uses the distorted-wave Born approximation and includes both ground-state and excited-state Ps formation [21]. Note that this prediction required an arbitrary scale factor of 0.5 to achieve agreement with the measurements.

For positron-impact ionization cross section measurements, the RPA is set to reject any positrons with energy loss *greater than* the ionization energy and this beam intensity is subtracted from the intensity of the beam when the RPA is set to transmit all positrons. The difference is proportional to the ionization cross section. As with other integral cross sections, the measurements provide absolute values. Figure 6 shows ionization cross section data for

Fig. 4. Integral cross section for the 6s 3/2 state of xenon compared with the predictions of a recent theory [27].

krypton, compared with two previous measurements made using a different method. This is an absolute comparison with no fitted parameters. There is very good absolute agreement up to about 35 eV but some disagreement above that energy, particularly for the data of Ref. [22]. This difference bears further scrutiny, both in its own right and also because it is used to determine positronium formation cross sections by the method described in Ref. [8].

4. Energy-resolved studies of positron annihilation – Feshbach resonances and bound states [23]

We designed and built a new experiment to make the first measurements of positron annihilation that are resolved as a function of positron energy, below the threshold for positronium atom formation (so-called "direct annihilation"). This experiment successfully addressed a four-decade old question as to the origin of very large annihilation rates observed in large molecules [3].

Conventionally, annihilation rates are expressed in terms of Z_{eff}, which is the annihilation rate per molecule normalized to the (Dirac) rate of annihilation for a positron in an uncorrelated electron gas. In particular, for a gas of atoms or molecules with number density n_m and electron density $n_m Z$; where Z is the number of electrons in the molecule, the normalized annihilation rate in this uncorrelated model is $Z_{eff} = Z$ [6]. In contrast, in experiments using a Maxwellian distribution of positrons at 300 K (i.e., $k_B T = 25 \, meV$), Z_{eff} for butane (C_4H_{10}) is 11,000 as compared with $Z = 34$, while for dodecane ($C_{12}H_{26}$), $Z_{eff} = 2 \times 10^6$, compared with $Z = 98$ [6]. Thus electron-positron correlations play a crucial role in the annihilation process in molecules. It is this long-standing puzzle that we set out to solve.

We found very large enhancements in Z_{eff} at energies in the range of the molecular vibrations and values of $Z_{eff} \sim Z$ for higher energies. This is illustrated in Fig. 7, which shows data for butane (C_4H_{10}; $Z = 32$) over a range of several electron Volts. The largest peak in the spectrum in all alkanes studied corresponds to the C–H stretch mode at 0.37 eV. Comparison of data for this peak in butane and fully deuterated butane (C_4D_{10}) demonstrated unequivo-
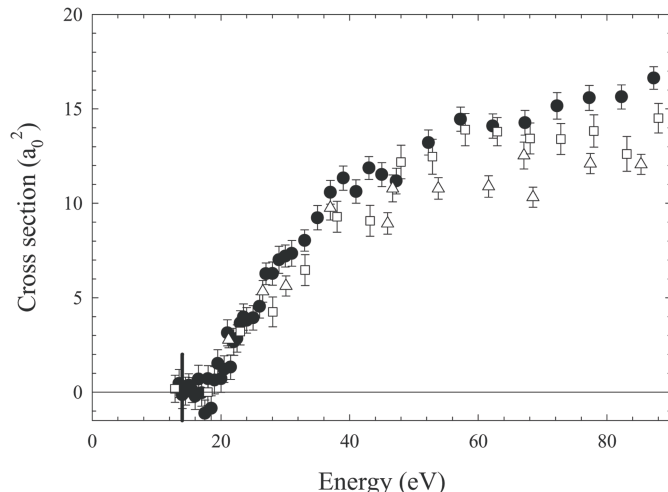
Fig. 7. Z_{eff} as a function of positron energy for butane (C_4H_{10}). Note the semi-log scale. $Z_{eff} \sim 100$ for energies larger than about 0.4 eV but rises $\sim$ two orders of magnitude at lower energies in the range of the molecular vibrations. The value of Z_{eff} for a Maxwellian distribution of positrons at 300 K (i.e., 25 meV) is 11,300.

cally that the resonant enhancements in Z_{eff} were due to the molecular vibrational modes [16]. Namely, when the spectra were scaled by the changes in energy of the modes expected for the change in effective mass, the position and shape of the C-H stretch peaks were virtually identical. Fig. 8 shows the low-energy portion of the spectrum of propane on an expanded scale and compared with the spectrum of linear vibrational modes of the molecule. Note the qualitative agreement between the spectrum of vibrational modes and the Z_{eff} spectrum.

We have now studied Z_{eff} for a range of molecules resolved as a function of positron energy. Small molecules studied include C_2H_2, C_2H_4, C_2H_6, and NH_3. We made a systematic study of alkane molecules C_nH_{2n+2}, for $n = 1 - 9$, and 12; 1-fluoropentane and 1-fluorononane and isopentane [23]. We have also made measurements of the noble gas atoms Ar and Xe, which both show values of $Z_{eff} \sim Z$. Shown in Fig. 9 are data for two alkanes. The main qualitative feature (which was unanticipated before

Fig. 6. Cross section for positron-impact ionization of krypton as a function of energy: (●) this work; (△) Ref. [22]; and (□) Ref. [29].

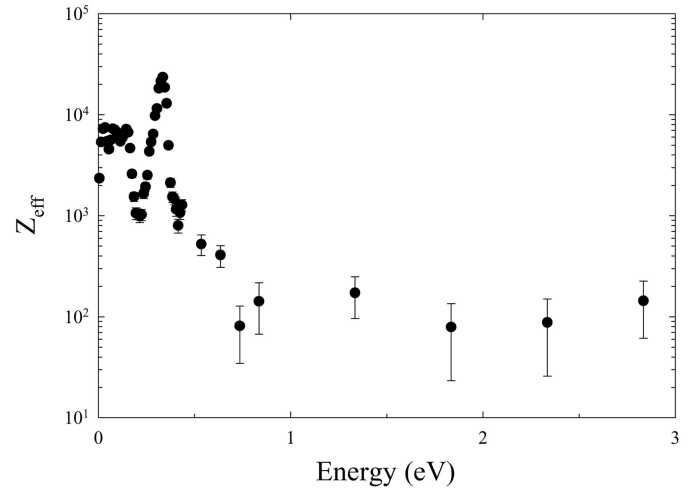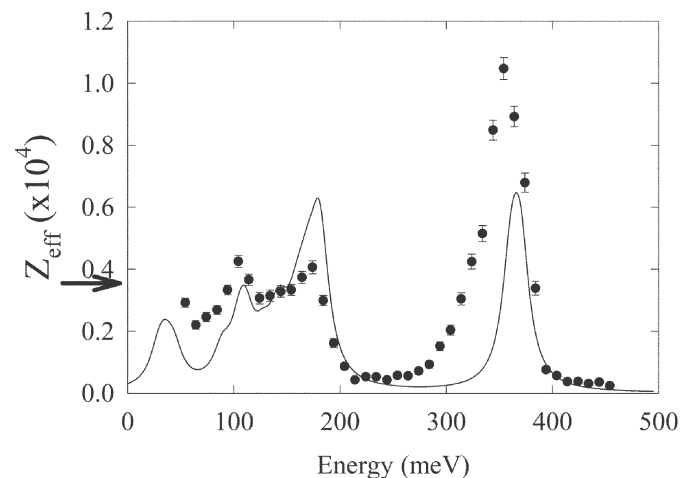*Fig. 8.* Z_{eff} as a function of positron energy for propane (C_3H_8) in the range of the molecular vibrations. Also shown (-) for comparison is the spectrum of linear vibrational modes in butane, broadened by a Lorentzian lineshape with a width of 10 meV and scaled arbitrarily. Note the similarity of the spectra. The horizontal arrow indicates the value of Z_{eff} for a Maxwellian distribution of positrons at 300 K (i.e., 25 meV).

the experiment), is a large enhancement in Z_{eff} at an energy downshifted from the C-H stretch mode frequency ($\varepsilon_{C\text{-}H} \sim 370\,\text{meV}$). As shown in Fig. 10, for alkanes ranging from methane to dodecane, the downshift, $\Delta\varepsilon$, increases as the number of carbons in the molecule increases. Values of Z_{eff} observed at the C-H peak are, in all cases, comparable to the value at 300 K, Z_{eff} (300 K), even though the magnitude of Z_{eff} varies by $> 10^4$. Generally, $Z_{eff}(\varepsilon)$ in the region of the molecular vibrations in alkanes is much greater than Z and reflects qualitatively the density of molecular vibrational states.

These data support the model, proposed previously [5,24] and recently developed in detail by Gribakin [7], that the large annihilation rates observed in molecules are due to vibrational Feshbach resonances. The model assumes there is a bound state of the positron and molecule. If the incident energy of the positron and the energy of binding are large enough to excite a vibrational mode, then the positron can become (temporarily) trapped on the molecule, greatly enhancing the electron-positron overlap and the resulting probability of annihilation. The energy shift, $\Delta\varepsilon$, is a measure of the positron binding energy. As a result, this experiment provides the first experimental measurement of positron binding to atoms or molecules. The fact that Z_{eff} (300 K) in all of the alkanes is comparable to $Z_{eff}(\varepsilon_{C\text{-}H})$, while the magnitude of both varies by many orders of magnitude, provides evidence that this resonance mechanism is also operative at 300 K.

Measurements at energies above the molecular vibrations (c.f., Fig. 9) show $Z_{eff} \sim Z$, providing further confirmation that the large values of Z_{eff} are due to vibrational resonances and not some phenomenon involving the electronic states. Many questions still remain regarding the details of this vibrational resonance mechanism, including the nature of the bound states and the redistribution of vibrational energy in the positron-molecule complex.
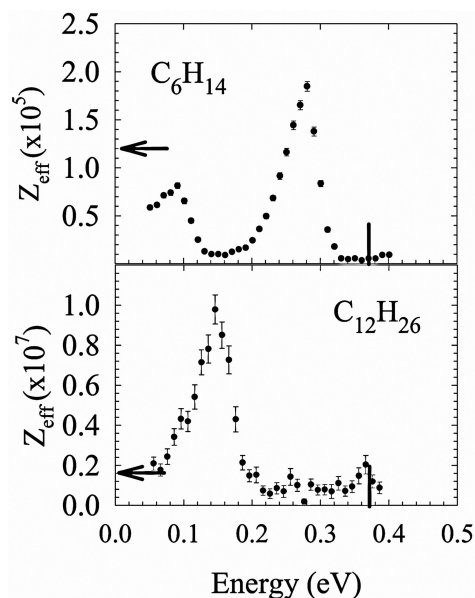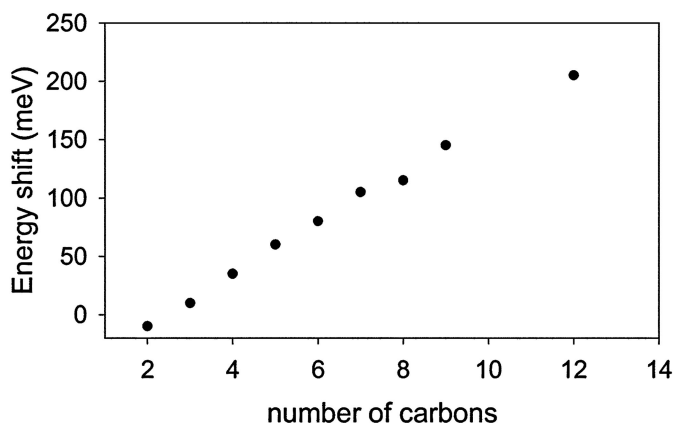

Fig. 10. Energy downshift, $\Delta\epsilon$, of the C-H stretch mode in alkane molecules as a function of number of carbon atoms in the molecule.

We now plan to address the wide range of outstanding issues by more detailed and comprehensive studies of Z_{eff} as a function of positron energy. Of particular interest is the spectacular chemical specificity of the effect. Fluoroalkanes have orders of magnitude smaller annihilation rates than do their hydrocarbon analogs. Substituting one fluorine in an alkane typically increases Z_{eff} for 300 K (25 meV) positrons [25], but decreases Z_{eff} at higher energies, at least in hexane and nonane, while the position of the C–H stretch peak appears to remain the same. See Ref. [23] for details.

5. Concluding remarks

We present here an overview of recent low-energy positron scattering and annihilation studies of atoms and molecules. The cold, trap-based beam and the technique of studying scattering in a magnetic field of variable strength allows us to address a number of questions of interest. The technique is particularly well suited to making high energy-resolution measurements; measuring integral, state-resolved cross sections; and investigating phenomena at low values of positron energy. In the scattering area, future emphasis will be placed on investigating low-energy and threshold phenomena.

The experiments described above to study low-energy positron annihilation in molecules answered a key question. The origin of large annihilation rates in hydrocarbons is the excitation of vibrational Feshbach resonances. These experiments provide evidence that positrons bind to hydrocarbon molecules. We interpret the fact that *fluorocarbons* have orders of magnitude smaller values of Z_{eff} as evidence that positrons do not bind to these molecules.

Still, a number of outstanding issues in the area of low-energy positron annihilation in molecules remain to be addressed. We would like to understand the role of chemical specificity and molecular shape (e.g., aromatics vs. chain hydrocarbons) in determining annihilation rates. Another interesting observation is the fact that one fluorine on a large alkane can change Z_{eff} by a significant factor, while the C–H stretch peak remains at the same position. Finally, it is of interest to develop a more quantitative connection between the Feshbach resonance model and the large values of Z_{eff} observed at 300 K.

Fig. 9. Data for annihilation rate, Z_{eff}, as a function of positron energy for two alkane molecules, hexane and dodecane. Note that Z_{eff} for the two molecules differs by a factor $\sim 10^2$. Horizontal arrows indicate the value of Z_{eff} (300 K). The large peaks correspond to the C-H stretch mode $\{\epsilon_{C\text{-}H} = 0.37\,\text{eV(vertical bar)}\}$, downshifted in energy by an amount that increases with molecular size.

As pointed out by Gribakin, [7] a number of different mechanisms could be operative in small molecules (e.g., $Z_{\text{eff}} \leq 10^3$). We have conducted some measurements for these species, e.g., the two-carbon hydrocarbons {e.g., C_2H_6, C_2H_4, and C_2H_2 [16]}, and more are in progress. Theoretical calculations for annihilation in these species would be most welcome.

Acknowledgements

References

1. Charlton, M. and Humberston, J. W., "Positron Physics" (Cambridge Univ. Press, Cambridge, 2001).
2. Surko, C. M., "New Directions in Antimatter Chemistry and Physics," (C. M. Surko and F. A. Gianturco, eds.) (Kluwer Scientific Publishers, the Netherlands, 2001).
3. Paul, D. A. L. and Saint-Pierre, L., Phys. Rev. Lett. **11**, 493 (1963).
4. Heyland, G. R. et al., Can. J. Phys. **60**, 503 (1982).
5. Surko, C. M. et al., Phys. Rev. Lett. **61**, 1831 (1988).
6. Iwata, K. et al., Phys. Rev. A **61**, 022719-1-17 (2000).
7. Gribakin, G. F., Phys. Rev. A **61**, 22720 (2000).
8. Laricchia, G. et al., J. Phys. B **35**, 1 (2002).
9. Sullivan, J., Gilbert, S. J. and Surko, C. M., Phys. Rev. Lett. **86**, 1494 (2001).
10. Sullivan, J. P. et al., Phys. Rev. Lett. **87**, 073201 (2001).
11. Schultz, P. J. and Lynn, K. G., Rev. Mod. Phys. **60**, 701 (1988).
12. Guessoum, N., Ramaty, R. and Lingenfelter, R. E., Astrophys. J. **378**, 170 (1991).
13. Hulett, L. D. et al., Chem. Phys. Lett. **216**, 236 (1993).
14. Murphy, T. J. and Surko, C. M., Phys. Rev. A **46**, 5696 (1992).
15. Sullivan, J. P. et al., Phys. Rev. A **66**, 042708-1-12 (2002).
16. Gilbert, S. J. et al., Phys. Rev. Lett. **88**, 0443201 (2002).
17. Gilbert, S. J., Greaves, R. G., and Surko, C. M., Phys. Rev. Lett. **82**, 5032 (1999).
18. Sullivan, J. P. et al., Nucl. Instum. Meth. Phys. Res. B **192**, 3 (2002).
19. Buckman, S. J., "New Directions in Antimatter Chemistry and Physics," (C. M. Surko and F. A. Gianturco, eds.) (Kluwer Scientific Publishers, the Netherlands), 413–35 (2001).
20. McAlinden, M. T. and Walters, H. R. J., Hyperfine Interact. **73**, 65 (1992).
21. Gilmore, S., McAlinden, M. T. and Walters, H. R. J., Unpublished (2003).
22. Kara, V. et al., J. Phys. B **30**, 3933 (1997).
23. Barnes, L. D., Gilbert, S. J. and Surko, C. M., Phys. Rev. A **67**, 032706 (2003).
24. Smith, P. M. and Paul, D. A. L., Can. J. Phys. **48**, 2984 (1970).
25. Iwata, K. et al., Phys. Rev. A **51**, 473 (1995).
26. Kimura, M. et al., Phys. Rev. Lett. **80**, 3936 (1998).
27. Parcell, L. A., McEachran, R. P. and Stauffer, A. D., Nucl. Inst. Meth. B **192**, 180 (2002).
28. Stein, T. S. et al., Hyperfine Interact. **73**, 53 (1992).
29. Moxom, J., Ashley, P. and Laricchia, G., Can. J. Phys. **74**, 367 (1996).